Article

Chinese Science Bulletin

Geochemistry

July 2013 Vol.58 No.20: 2473–2479
doi: 10.1007/s11434-013-5756-8

In-situ cosmogenic ^{36}Cl denudation rates of carbonates in Guizhou karst area

XU Sheng[1,2], LIU CongQiang[1*], FREEMAN Stewart[2], LANG YunChao[1], SCHNABEL Christoph[2], TU ChengLong[1], WILCKEN Klaus[2] & ZHAO ZhiQi[1]

[1] *State Key Laboratory of Environmental Geochemistry, Institute of Geochemistry, Chinese Academy of Sciences, Guiyang 550002, China;*
[2] *Scottish Universities Environmental Research Center, East Kilbride, G75 0QF, UK*

Received December 23, 2012; accepted January 21, 2013; published online March 13, 2013

This study quantifies surface denudation of carbonate rocks by the first application of in-situ cosmogenic ^{36}Cl in China. Concentrations of natural Cl and *in-situ* cosmogenic ^{36}Cl in bare carbonates from Guizhou karst areas were measured with isotope dilution by accelerator mass spectrometer. The Cl concentration varied from 16 to 206 ppm. The ^{36}Cl concentrations were in range of $(0.8–2.4)\times10^6$ atom g^{-1}, resulting in total denudation rates of 20–50 mm ka^{-1} that averaged over a 10^4–10^5 a timescale. The ^{36}Cl-denudation rates showed roughly a negative correlation with the local mean temperature. This preliminary observation may suggest the variations of proportions of chemical weathering and physical erosion in denudation process, depending upon local climatic conditions.

***in-situ* cosmogenic ^{36}Cl, denudation rate, climatic condition, carbonate, Guizhou**

Citation: Xu S, Liu C Q, Freeman S, et al. *In-situ* cosmogenic ^{36}Cl denudation rates of carbonates in Guizhou karst area. Chin Sci Bull, 2013, 58: 2473–2479, doi: 10.1007/s11434-013-5756-8

Estimation of denudation rates in karst area is one of the basic subjects to study the role of carbonate rock weathering in the global carbon cycle and evolution of the local landscapes [1,2]. Since Corbel [3] presented a method to estimate regional erosion rate by precipitations and average solved matter in water, many other direct measurement and indirect estimation methods have been presented. These mainly include (1) observation of solute load based on hydrochemical compositions [4,5]; (2) weight loss records of limestone tablets exposed in different environments [2,6]; (3) measurements on the exposed surfaces with microerosion meters [7,8]; (4) measurements of height of pedestals in exposed surface [5,9]; and (5) estimation with in situ cosmogenic nuclides ^{36}Cl (half-life 301 ka) [10,11]. Of these, method of in situ cosmogenic ^{36}Cl is considered advantageous as it records the history of long-term erosion and can minimize the uncertainty caused by the extrapolation problems that other methods need to consider. Although applications of *in situ* cosmogenic ^{36}Cl mainly focused on the surface exposure history, few pioneering studies have indicated the validity of in situ cosmogenic ^{36}Cl for the estimation of denudation rates in karst areas [10,11]. For instance, Stone et al. [10] estimated ^{36}Cl denudation rates from limestone in Australia, ranging from 1 mm ka^{-1} in arid area to 150 mm ka^{-1} in tropic area. Matsushi et al. [11] reported ^{36}Cl denudation rates of calcite in Japanese island in range of 20–60 mm ka^{-1}. These studies presented that the denudation rate of carbonates is mainly controlled by the local climates. To further clarify this conclusion, we used *in-situ* cosmogenic ^{36}Cl to study long-term erosion in subtropic Guizhou karst area, SW China and subsequently to compare with other short-term estimations.

In southwest China, a variety of serious environmental issues are recently presented. This mainly includes issues of water and land use, acid rain and karstification all of which are associated with the denudation of carbonate weathering [12]. Guizhou Province is located in the center of the Southeast Asian Karst Region where karstification is most

*Corresponding author (email: liucongqiang@vip.skleg.cn)

developed in the world. It is also featured by the most diverse karst types and the largest karst area in the world. In Guizhou, carbonate rocks occupy ~62% land surface, of which limestone and dolomite are the major rock types. Modern climate in Guizhou is in catalogue of subtropic monsoon zone with average annual precipitation of 900–1300 mm. The large elevation gradient of the Guizhou Province, about 2800 m above see level (m a.s.l.) in west and about 500 m a.s.l. in east, results in low mean temperature in west (11–12°C) and high in east (15–17°C). The carbonate strata exposed are mainly Pre-Jurassic in age, including Permian and Triassic carbonate rocks within the catchment of Rivers Wujiang, Qingshuijiang and Wuyanghe. None of these rocks shows evidence of later burials including glaciation.

1 Materials and methods

Six bare carbonate samples were collected from Guizhou karst areas (Figure 1). Details of the sampling locations together with other parameters are shown in Table 1. The surface samples are from outcrops on open hilltops so as to avoid recent soil cover and to be as representative as possible of the surrounding landscape. In field, samples (~1 kg) were collected from the top surface (2–5 cm) of the exposed carbonate rocks. Effect of snow shielding on in situ cosmogenic ^{36}Cl accumulation can be considered minimal as the amount and period of annual snow accumulation under local climatic conditions is not great. In addition to effects from soil and glacier cover, care was also taken to judge non-disturbance by human activities. Figure 2 shows landscape of each sampling locations.

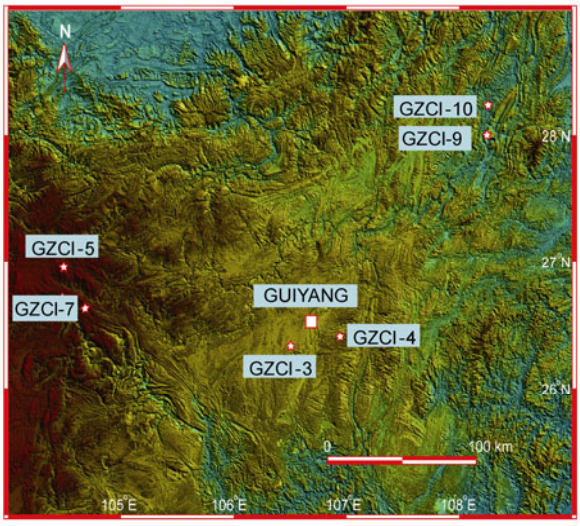

Figure 1 Map showing sample locations and landscapes in Guizhou karst area.

The rock samples were firstly crushed and the sieved 0.25–0.125 mm fraction was used for Cl and ^{36}Cl preparation and measurement. Major and trace elemental compositions were analyzed by ICP-MS at the State Key Laboratory of Environmental Geochemistry, Institute of Geochemistry, Chinese Academy of Sciences.

Chemical extractions and measurements of natural Cl and *in-situ* ^{36}Cl were carried out at Scottish Universities Environmental Research Centre (SUERC). Two rounds of 2 mol L^{-1} HNO_3 leaching eliminated the meteoric ^{36}Cl and any possible contaminants by removing ~10% of the grain surfaces. Subsequently, the treated samples were dissolved by 8 mol L^{-1} HNO_3 and filtered. The residues were normally about <3% of the total sample mass, indicating minor silicate minerals. About 1–2 mg Cl of the ^{35}Cl-enriched spike solution with $^{37}Cl/^{35}Cl$ 0.051 was added in the filtered acidic solution. A nature Cl carrier was also added into the chemical blank sample. AgCl precipitate can be obtained by adding 10% $AgNO_3$ solution and was then centrifuged. The centrifuged AgCl was re-resolved by adding HNO_3 solution. In order to minimize interference from isobar ^{36}S, $Ba(NO_3)_2$ was added to make $BaSO_4$ precipitation. After 48 h settlement, $BaSO_4$ precipitates were centrifuged. More $AgNO_3$ solutions were then added in the remaining solution to get AgCl precipitation again. The precipitated AgCl was washed and finally dried at 90°C for 12 h. Following the same procedure, chemical blank samples including ^{35}Cl-enriched spike and natural Cl were also prepared.

The dried AgCl was pressed into a specific Cu sample holder for AMS analysis. The sample holder design for ^{36}Cl measurement is slightly different from the other nuclides. They are made of copper and twice the size of the "normal" sample holder design. With this design, S-free AgBr (99.9%) is firstly pressed into 6 mm diameter sample holder and subsequently the precipitated AgCl are pressed into the

Table 1 Samples for *in-situ* cosmogenic ^{36}Cl measurement from Guizhou

Sample	Locality	Material	Altitude (m a.s.l.)	Longitude & latitude	Density (g cm^{-3})	Mean temperature (°C)	Annual precipitation (mm a^{-1})
GZCl-3	Pingba	limestone	1226	26°24.972′E, 106°31.718′N	2.74	15	1150
GZCl-4	Longli	dolomite	1110	26°28.549′E, 106°57.866′N	2.82	14	1050
GZCl-5	Hezhang	limestone	2329	26°58.456′E, 104°31.100′N	2.11	12	900
GZCl-7	Liupanshui	limestone	1959	26°41.863′E, 104°42.609′N	2.69	11	1250
GZCl-9	Sinan	limestone	586	27°52.806′E, 108°18.228′N	2.63	17	1150
GZCl-10	Dejiang	limestone	577	28°05.859′E, 108°19.331′N	2.31	15	1180

Figure 2 Photos showing landscape of sample locations in Guizhou karst area.

center (with 1 mm diameter) of AgBr bed so as to minimize S extractions from Cu. The samples were measured for natural Cl and ^{36}Cl with the 5 MV accelerator mass spectrometer (AMS) at SUERC. The terminal voltage was set at 5 MV and argon gas stripping to the 5+ charge state (Cl^{5+}) was selected. Both ^{35}Cl and ^{37}Cl signals are measured with high-energy off-axis Faraday cups. High-energy current measurements are preferred because the charge sensitive amplifiers at the high-energy end of the accelerator are better quality than our low energy integrators. Also possible molecular interferences are be dissociated in the stripper. Details of the AMS measurement procedure can be referred in [13].

Natural Cl content in rock was calculated by conventional isotope dilution. Such a method allows us to determine simultaneously Cl and ^{36}Cl with a single sample preparation, which can significantly reduce the sample process times and the total uncertainty of analysis. The content of Cl in a spiked sample is calculated by

$$[\mathrm{Cl}]_{\mathrm{sample}} = [\mathrm{Cl}]_{\mathrm{spike}} \cdot \frac{1+R_{\mathrm{sample}}}{1+R_{\mathrm{natural}}} \cdot \frac{R_{\mathrm{sample}}-R_{\mathrm{spike}}}{R_{\mathrm{natural}}-R_{\mathrm{sample}}}, \quad (1)$$

where $[\mathrm{Cl}]_{\mathrm{sample}}$ and $[\mathrm{Cl}]_{\mathrm{spike}}$ are Cl concentrations in sample and spike solution, respectively. R_{sample}, R_{spike} and R_{natural} are measured ^{37}Cl/^{35}Cl ratios in sample, spike and nature, respectively.

^{36}Cl concentration was calculated by AMS-measured ^{36}Cl/Cl ratio normalized using a standard with the ^{36}Cl/Cl ratio of 1.6×10^{-12} and natural ^{37}Cl/^{35}Cl ratio [14]. ^{36}Cl ions can be separated from isobar ^{36}S at the final detector with a 30 nm thickness SiN membrane window, resulting in the background ^{36}Cl/Cl ratio less than 1×10^{-15}. The ^{36}Cl/Cl isotope ratio for the samples was typically in range of 10^{-13}. Long-term repeat measurements of the secondary standard with ^{36}Cl/Cl ratio of 5×10^{-13} result in 3% precision.

2 Results and discussion

Chemical compositions of major and trace elements in carbonates are listed in Table 2. The mole Ca/Mg ratios ranging from 2 to 140 indicate that rock types of carbonates in this study are from pure calcite to dolomite. Sample GZCL-7 contains 40% Ca and thus indicates a pure calcite. Sample GZCL-4 has the lowest Ca and the highest Mg concentrations, belonging to the catalogue of typical dolomite.

Table 2 Chemical compositions of major and trace elements in carbonates from Guizhou

Sample	Ca (%)	Mg (%)	K (ppm)	Na (ppm)	Mn (ppm)	Fe (ppm)	Li (ppm)	Sm (ppm)	Gd (ppm)	U (ppm)	Th (ppm)	Ca/Mg (mol)
GZCl-3	33.7	0.2	249	48.2	23.6	517.4	0.721	0.156	0.252	1.55	0.183	110
GZCl-4	24.8	7.3	886	72.3	20.8	794.5	2.050	0.226	0.165	0.284	0.471	2
GZCl-5	35	0.16	286	22.9	40.8	373.8	0.269	0.221	0.285	0.352	0.174	142
GZCl-7	40.8	0.24	66	50.7	21.9	163.2	0.453	0.0384	0.0857	1.64	0.047	111
GZCl-9	36.5	0.29	8	11	23.9	148.4	0.430	0.0884	0.108	0.345	0.0645	82
GZCl-10	33	0.43	573	45.7	120.3	720	1.140	0.135	0.179	0.823	0.287	50

Concentrations of natural Cl and *in-situ* cosmogenic nuclide ^{36}Cl in carbonate are listed in Table 3. Cl concentrations vary from 16 to 206 ppm, whereas ^{36}Cl rang in (0.8–2.4)×10^6 atom g^{-1}. Cl and ^{36}Cl concentrations in two duplicate samples (GZCl-4 and GZCl-5) are consistent within the error margin of 1σ. Again, sample GZCL-4 has the highest Cl concentration (206 ppm), obviously higher than other samples (16–95 ppm).

Calculation of ^{36}Cl-denudation rates essentially requires information of ^{36}Cl production routes and rates in carbonate rocks. It is widely accepted that cosmogenic ^{36}Cl can be mainly produced in carbonates by reactions:

(1) spallation of heavy nuclei Ca and K;

(2) μ^- capture in ^{40}Ca via reactions ^{40}Ca (μ^-,n)^{36}Cl and ^{40}Ca(μ^-, $\nu_\mu\alpha$)^{36}Cl;

(3) spallogenic neutron capture in ^{35}Cl via reaction ^{35}Cl(n, γ)^{36}Cl;

(4) muon-genic neutron capture in ^{35}Cl via reaction ^{35}Cl(n, γ)^{36}Cl;

(5) nucleogenic ^{36}Cl by U and Th fission.

Thus, ^{36}Cl production rates in the carbonates at surface primarily depend on chemical compositions of target elements (i.e. Ca, K, Cl) and neutron absorbers (B, Sm, Gd, etc.), in addition to intensity of secondary cosmic ray that is dependence on the geomorphologic location. Cosmogenic ^{36}Cl accumulation in rocks (C) can be expressed as [10]

$$\frac{\partial C(x,t)}{\partial t} = P(x) - C(x,t)\lambda - \varepsilon\frac{\partial C(x,t)}{\partial x}, \tag{2}$$

where $P(x)$ is the total ^{36}Cl production rate as a function of depth (x). λ is the ^{36}Cl decay constant and ε the erosion rate (assuming both P and ε constant through exposure time t). Eq. (2) can be further integrated with $P(x)$ set according to the proportions of spallogenic and muongenic production rates.

$$C = C_0 e^{-\lambda t} + \frac{P_n}{\rho\varepsilon/\wedge_n + \lambda}\cdot e^{-\frac{\rho x}{\wedge_n}}\cdot\left(1 - e^{-\left(\lambda+\frac{\varepsilon\rho}{\wedge_n}\right)t}\right) + \frac{P_{\mu^-}}{\rho\varepsilon/\wedge_{\mu^-} + \lambda}\cdot e^{-\frac{\rho x}{\wedge_{\mu^-}}}\cdot\left(1 - e^{-\left(\lambda+\frac{\varepsilon\rho}{\wedge_{\mu^-}}\right)t}\right), \tag{3}$$

where C_0 is the initial ^{36}Cl concentration. P_n and P_μ are the ^{36}Cl production rates at surface by neutrons and muons, respectively. ρ is the density of rock, and $\wedge_n$ and $\wedge_\mu$ are penetration length for neutrons (160 g cm^{-2}) and muons (1300 g cm^{-2}), respectively. As an example, calculated equilibrium depth profile of ^{36}Cl with zero erosion for sample GZCl-7 is shown in Figure 3. The spallogenic production dominates near surface, whereas the muon induced production becomes dominant at intermediate depths.

Geological evidences indicate that carbonates in Guizhou karst area were exposure at surface since Jurassic [12]. Such a long-term surface exposure has most likely resulted in a steady-state of *in-situ* cosmogenic ^{36}Cl in the carbonates that have no later burial history. This is general true in Guizhou karst area, in particular in sample sites of this study. Thus, the denudation rates are calculated from steady-state solution to eq. (3). That is, if the samples had neglected initial ^{36}Cl concentration and were exposure at surface for a long period (i.e. indefinite), then eq. (3) can be simplified as

$$C = \frac{P_n}{\rho\varepsilon/\wedge_n + \lambda} + \frac{P_{\mu^-}}{\rho\varepsilon/\wedge_{\mu^-} + \lambda}. \tag{4}$$

A series of calibration studies have established the spallogenic and muongenic ^{36}Cl production system in carbonate rocks [15–18]. Accordingly the ^{36}Cl production rates in this study were calculated based on the chemical compositions of the carbonate rock (Tables 2 and 3), and scaled by using

Table 3 *In-situ* cosmogenic ^{36}Cl production rates and denudation rates of surface carbonates in Guizhou

Sample ID	Sample weight (g)	Spike Cl (mg)	Cl (ppm)	^{36}Cl[a] (10^6 atom g^{-1})	Surface production rates (atom g^{-1} a^{-1})[b]				Denudation rate[c] (mm ka^{-1})
					$P_{Ca\ spallation}$	$P^{35}{}_{Cl(n,\gamma)}{}^{36}Cl$ spallogenic netrons	$P^{40}{}_{Ca(\mu^-,\alpha)}{}^{36}Cl$	$P^{35}{}_{Cl(n,\gamma)}{}^{36}Cl$ muon-genic netrons	
GZCl-3	22.1	1.702	17.5	0.793	27.1	4.0	2.9	0.3	44
GZCl-4	21.9	1.695	205.6	2.36	18.4	47.1	2.8	3.8	40
	22.2	1.705	206.7	2.30					
GZCl-5	22.6	1.684	16.2	2.22	61.3	8.0	4.8	0.4	41
	22.1	1.706	16.8	2.32					
GZCl-7	21.9	1.684	46.0	1.77	54.8	16.4	4.0	1.0	47
GZCl-9	22.1	1.691	21.7	1.41	18.8	3.1	2.2	0.3	17
GZCl-10	21.8	1.702	94.9	2.02	17.3	14.1	2.3	1.3	19

a) Subtracted from nucleogenic ^{36}Cl from U and Th; b) adjusted for sample latitude, altitude, thickness, horizon and target composition; c) ~10% overall uncertainty.

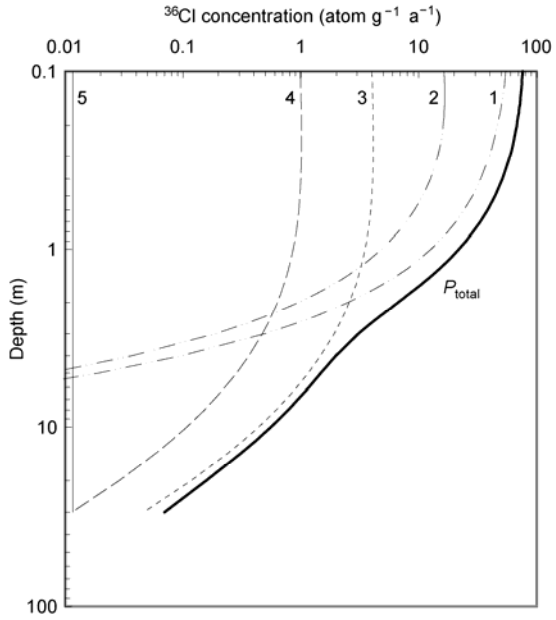

Figure 3 Calculated equilibrium depth profile of ^{36}Cl with zero erosion for sample GZCl-7. The spallogenic production dominates near surface, whereas the muon induced production becomes dominant at intermediate depths. 1, Ca spallation; 2, ^{35}Cl(n, γ)^{36}Cl (spallogenic neutron); 3, ^{40}Ca (μ^-, α)^{36}Cl; 4, ^{35}Cl (n, γ)^{36}Cl (μ^- produced neutron); 5, ^{35}Cl(n, γ)^{36}Cl (nucleogenic neutron).

geographic information (latitudes and altitudes) of individual locations. Subsequently, the ^{36}Cl-denudation rates of the carbonate rocks were calculated by an inverse analysis which is an iterative computation searching for the denudation rates that mostly match the observed ^{36}Cl concentrations [11,16]. As a result, the calculated ^{36}Cl-denudation rates in this study vary from 20 to 50 mm ka^{-1} (Table 3). As stated above, these were long-term denudation rates averaged the timescale of 10^4–10^5 a during which both chemical weathering and physical erosion processes removed a few meters of surface carbonate rocks.

In comparison with other ^{36}Cl-denudation rates, the denudation rates of Guizhou carbonate rocks are intermediate between those in dry temperate southeast Australia (~20 mm ka^{-1}) and tropical Papua New Guinea (>150 mm ka^{-1}) [10], and comparable with those in subtropical to subarctic regions in Japan (20–60 mm ka^{-1}) [11]. The ^{36}Cl-denudation rates in Guizhou are also comparable with other long-term estimates obtained by height changes of pedestals beneath glacial erratics on a pavement, i.e. Yorkshire, UK (3–13 mm ka^{-1}) [19]; Maren Mountains, Switzerland (15 mm ka^{-1}) [20]; West Irian, Indonesia (32 mm ka^{-1}) [21]; Leitrim, Ireland (42 mm ka^{-1}) [22] and Patagonia (40–75 mm ka^{-1}) [23]. However, they are much lower than that from tsunami remains on raised coral-reef terraces in Kikaijima, Japan (205 mm ka^{-1}) [24]. The regional differences in denudation rates can be reasonably considered as variable local factors such as climatic conditions, tectonics and physical properties of carbonate rock. However, due to limited data, further discussion of the worldwide variation in denudation rates of carbonate rock is beyond this study.

Although this study is preliminary, the most obvious feature in this study is that the ^{36}Cl denudation rates are high in the western and central Guizhou highlands (40–47 mm ka^{-1}) and low in the eastern lowlands (17–19 mm ka^{-1}). No correlation between denudation rate and rock properties (rock type and density) was observed, suggesting minimal lithogological effect. Hence, such a regional variation in denudation rates is likely controlled by climatic differences between the sites. Figure 4 shows relationship between ^{36}Cl-denudation rates and local climatic factors (annual precipitation and mean temperature). Obviously, there is no clear correlation between denudation rate and annual precipitation (Figure 4(a)). However, a weak negative correlation between denudation rate and mean temperature with correlation coefficient r=0.76 can be observed in Figure 4(b). As the ^{36}Cl denudation rates averaged a long-term timescale of 10^4–10^5 a, it may be inappropriate to combine the denudation rates with the present climate factors.

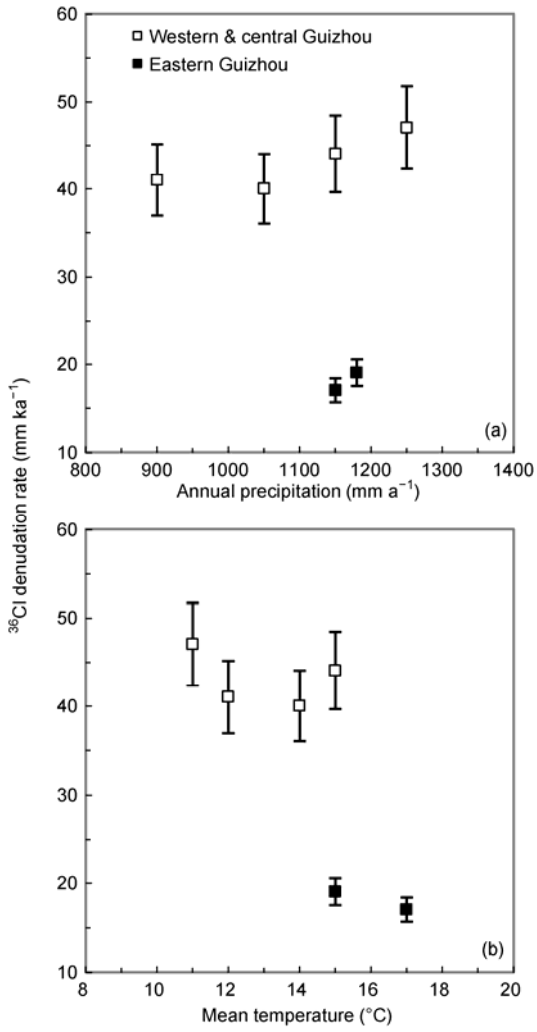

Figure 4 Correlation between denudation rate and climate factors.

Matsushi et al. [11] suggested the validity of combination of the long-term ^{36}Cl denudation rates with the present climatic factors based on studies of the Japanese carbonate rocks.

By normalizing with annual precipitation (L cm^{-2} a^{-1}) to exclude the annual precipitation influence on denudation, Matsushi et al. [11] treated the denudation rates (mg cm^{-2} a^{-1}) of Japanese carbonates by an Arrhenius-plot of mean temperature (K) (Figure 5). The dotted line in the Arrhenius-plot represents chemical dissolution with apparent activation energy of 60 kJ mol^{-1}, which is comparable to 16.2–63 kJ mol^{-1} obtained in calcite dissolution experiments in the laboratory, as discussed in [11]. Thus, the Japanese samples distributed along the chemical dissolution line were mainly resulted from the contribution of chemical weathering (dissolution) to total denudation [11]. In colder regions (i.e. mean temperatures below 15°C), the Japanese samples had elevated denudation rates and scattered above the dissolution line. As the increase in denudation rates was found to associate with the occurrence of freeze-thawing days in Japan, it was suggested that the physical erosion significantly contributed to the total denudation rate [11]. Following the treatment and discussion proposed in [11], two samples from the eastern Guizhou lowlands plotted around the dissolution line suggest that chemical weathering mainly contributed the total denudation. However, like most Japanese carbonates, samples from the western and central Guizhou highlands scattered above the dissolution line. This implies that the physical erosion plays an important role on total denudation in addition to chemical weathering. If the chemical weathering rate was ~20 mm ka^{-1}, the physical erosion rates would take 50%–60% in total denudation in the western and central Guizhou highlands.

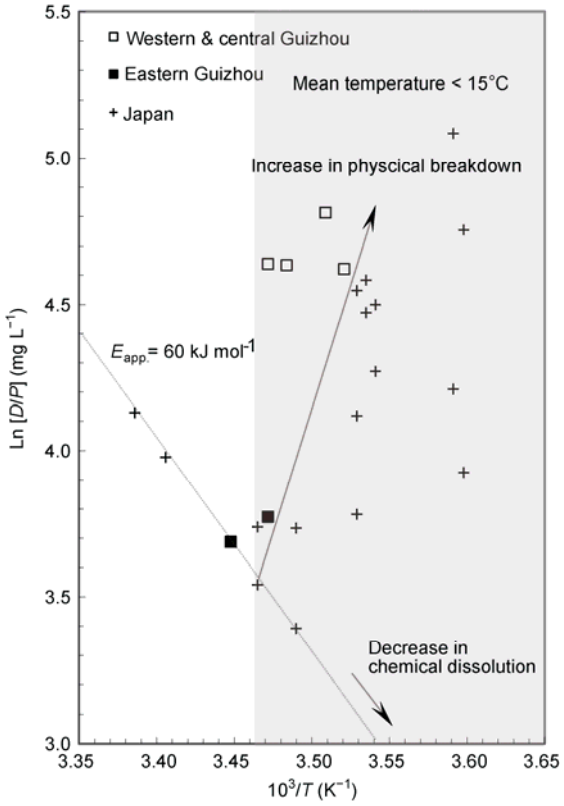

Figure 5 Arrhenius-plot with mean temperature (T) for denudation rates (D) normalized with annual precipitation (P). The dotted line denotes chemical dissolution with apparent activation energy of 60 kJ mol^{-1}, whereas the solid line represents a trend of enhanced physical erosion within the cooler region below ~15°C (shaded region).

As our samples were mainly collected within the catchment of the Wujiang River, it is worthy to compare ^{36}Cl denudation rates with other methods. Han and Liu [12] presented carbonate chemical erosion rates from three major rivers in Guizhou by systematic measurements of water chemical compositions, 49, 57 and 43 mm ka^{-1} in Wujiang, Wuyang and Qingshui rivers, respectively. These values are obviously higher than the chemical weathering rates (~20 mm ka^{-1}) deduced by ^{36}Cl. As the cosmogenic ^{36}Cl denudation rate reflects a relative long-term scale (10^4–10^5 a), the distinct chemical weathering rates imply a recent shift on weathering conditions. At present, we do not have a convincing explanation for this interesting discrepancy. However, two possibilities could be considered. First, human activity might have recently enhanced carbonate rock weathering. Alternatively, the high carbonate weathering rates deduced from the water chemistry may only reflect a result of carbonate rock-atmosphere interactions. Further ^{36}Cl measurements of surface and profile carbonate samples, together with ^{10}Be and/or ^{26}Al measurements of potential silicate rocks, will be helpful to clarifying these alternatives. In particular, the ^{36}Cl profiles can be expected to provide significant information to understand if and when the denudation rates have changed within last 10^4–10^5 a.

3 Conclusions

This study is the first application of *in-situ* cosmogenic ^{36}Cl to estimate denudation rates of carbonate rocks in China. The preliminary ^{36}Cl-denudation rates of 20–50 mm ka^{-1} were obtained in Guizhou karst area. Comparison of the ^{36}Cl-denudation rate and modern climatic factors suggests that chemical dissolution is the essential process for carbonate weathering, whereas physical erosion may become dominant in cooler conditions by freeze-thaw alteration which may enhance mechanical disintegration of rock surfaces. More ^{36}Cl measurements of carbonates together with ^{10}Be and/or ^{26}Al analyses of silicates in surrounding areas are needed to further clarify the physical erosion and chemical weathering process.

We thank Gu Fu and Li Longbo for field assistance, A. Dougans and L. Miguens-Rodriguez for laboratory assistance. This work was supported by the National Natural Science Foundation of China (41130536 and 41021062) and the State Key Laboratory of Environmental Geochemistry, Institute of Geochemistry, Chinese Academy of Sciences (9014).

1 Liu Z H. New progress and prospects in the study of rock-weathering-related carbon sinks (in Chinese). Chin Sci Bull (Chin Ver), 2012, 57: 95–102
2 Zhang C. Carbonate rock dissolution rates in different landuses and their carbon sink effect. Chin Sci Bull, 2011, 56: 3759–3765
3 Corbel J. Vitesse de l'erosion. Zeitschrift fur Geomorphologie, 1959, 3: 1–2
4 Gunn J. Limestone solution rates and processes in the Waitomo district, New Zealand. Earth Surf Proc Landforms, 1981, 6: 427–445
5 Plan L. Factors controlling carbonate dissolution rates quantified in a field test in the Austrian Alps. Geomorphology, 2005, 68: 201–212
6 Trudgill S T. Measurements of erosional weigth loss of rock tablets. Brit Geomorph Res Gr Tech Bull, 1975, 17: 13–19
7 High C, Hanna G K. A method for the direct measurement of erosion of rock surfaces. Brit Geomorph Res Gr Tech Bull, 1970, 5: 24
8 Cucchi F, Forti F, Furlani S. Lowering rates of limestone along thewestern Istrian shoreline and the Gulf of Trieste. Geogr Fisica Din Quat, 2006, 29: 61–69
9 Bögli A. Karst Hydrologyand Physical Speleology. Berlin-Heidelberg: Springer, 1980
10 Stone J, Allan G L, Fifield L K, et al. Limestone erosion measurements with cosmogenic chlorine-36 in calcite—Preliminary results from Australia. Nucl Instr Meth B, 1994, 92: 311–316
11 Matsushi Y, Sasa K, Takahashi T, et al. Chlorine-36 in calcite: Denudation rates of karst landform in Japan. Nucl Instr Meth B, 2010, 168: 1205–1208
12 Han G, Liu C Q. Water geochemistry controlled by carbonate dissolution: A study of the river waters draining karst-dominated terrain, Guizhou Province, China. Chem Geol, 2004, 204: 1–21
13 Wilcken K M, Freema S, Dougans A, et al. Improved ^{36}Cl AMS at 5 MV. Nucl Instr Meth B, 2010, 268: 748–751
14 Sharma P, Kubik P W, Fehn U, et al. Development of ^{36}Cl standards for AMS. Nucl Instr Meth B, 1990, 52: 410–415
15 Stone J O, Allan G L, Fifield L K, et al. Cosmogenic chlorine-36 from calcium spallation. Geochim Cosmochim Acta, 1996, 60: 679–692
16 Stone J, Evans J, Fifield L, et al. Cosmogenic chlorine-36 production in calcite by muons. Geochim Cosmochim Acta, 1998, 62: 433–454
17 Stone J. Air pressure and cosmogenic isotope production. J Geophys Res, 2000, 105: 23753–23759
18 Alfimov V, Ivy-Ochs S. How well do we understand production of ^{36}Cl in limestone and dolomite? Quat Geochron, 2009, 4: 462–474
19 Goldie H S. Erratic judgements: Re-evaluating solutional erosion rates of limestones using erratic-pedestal sites, including Norber, Yorkshire. Area, 2005, 37: 433–442
20 Bögli A. Karrentische, ein Beitrag zur Karstmorphologie. Zeits Geomorph, 1961, 5: 185–193
21 Peterson J A. Limestone pedestals and denudation estimates from Mt. Jaya, Irian Jaya. Aust Geogr, 1982, 15: 170–173
22 Williams P W. Limestone pavements with special reference to Western Ireland. Inst Brit Geogr Trans, 1966, 40: 155–171
23 Maire R, Esperanza E, Pernette J F, et al. Les 'glaciers de marbre' de Patagonie, Chili. Karstologia, 1999, 33: 25–40
24 Matsukura Y, Maekado A, Aoki H, et al. Surface lowering rates of uplifted limestone terraces estimated from the height of pedestals on a subtropical island of Japan. Earth Surf Proc Landforms, 2007, 32: 1110–1115